# Triphenylamine−Fluorene Alternating Conjugated Copolymers with Pendant Acceptor Groups: Synthesis, Structure−Property Relationship, and Photovoltaic Application

**Zhi-Guo Zhang,[†,‡] Ke-Li Zhang,*[,†] Gang Liu,[‡] Chun-Xiang Zhu,[§] Koon-Gee Neoh,[‡] and En-Tang Kang*[,‡]**

*College of Chemistry and Molecular Sciences, Wuhan University, Wuhan 430072, People's Republic of China, and Departments of Chemical & Biomolecular Engineering and Electrical & Computer Engineering, National University of Singapore, Kent Ridge, Singapore 119260*

*Received February 3, 2009; Revised Manuscript Received February 23, 2009*

ABSTRACT: Three triphenylamine−fluorene alternating conjugated copolymers, differing only in the aldehyde (**PTCHO**), monocyano (**PTCN**), and dicyano (**PTDCN**) pendant acceptor groups, have been designed and synthesized. The structures and properties of the conjugated copolymers were characterized by $^1$H NMR, elemental analysis, gel permeation chromatography (GPC), thermal gravimetric analysis (TGA), UV−visible absorption spectroscopy, photoluminescence (PL) spectroscopy, and cyclic voltammetry (CV). Through manipulating the acceptor attached to the same $\pi$-conjugated backbone, the electronic properties and energy levels of the copolymers were effectively tuned for blue, yellowish-green, and yellowish-orange emissions, resembling those of the primary colors. The effect of substituent on the electronic structure of the copolymers was also studied by molecular simulation. The blue shift in the $\pi$-$\pi$* transition of the backbone was associated with the variation in the structural geometry, whereas the charge transfer, excimer formation, and energy level variation were governed by the electron density distribution. The results suggest a simple and effective approach for tuning the emission in a conjugated polymer through modification of the pendant acceptor groups. In combination with a soluble fullerene (PCBM), **PTCN** and **PTDCN** were also used in the fabrication of bulk-heterojunction photovoltaic cells. The structure−property relationships revealed by the present copolymers are useful for the rational design of electroactive polymers for photoelectronic applications.

## 1. Introduction

Soluble conjugated polymers have received considerable attention because they can be processed in simpler and more cost-effective ways than their inorganic semiconductor counterparts. Their electronic and optical properties can be tuned via molecular design and synthesis.[1] In semiconductors, the transport of holes and electrons are governed by the HOMO (highest occupied molecular orbital) and LUMO (lowest unoccupied molecular orbital) energy levels. The energy levels of an organic semiconductor govern the efficiency of carrier injection and extraction,[2,3] control the energy and electron transfer processes at the heterojuction,[4] and determine the intrinsic photophysical properties, such as absorption and emission.[5−9] Therefore, the performance of conjugated semiconducting polymers can be optimized through fine-tuning of the energy levels via molecular design and engineering.

The opto-electronic properties of conjugated polymers can be efficiently tuned by intramolecular charge transfer involving donor−acceptor (D−A) interactions.[10,11] The hybridization of HOMO located on the donor moiety with LUMO located on the acceptor moiety provides a means for tuning the electronic and optoelectronic properties in device applications, such as light-emitting diodes,[12−15] photovoltaic cells,[16−19] field-effect transistors,[20−22] and memory devices.[23,24]

Commercially available triphenylamine−fluorene alternating conjugated polymers (PFTs) have been widely used as donor materials for probing device mechanism and performance or for fabricating state-of-the-art semiconductor devices and taking advantage of their unique properties, such as high hole mobility and solution processability.[25−30] In this work, we demonstrate effective tuning of energy levels and PL in PFTs by coupling of appropriate pendant acceptor groups. Furthermore, the potential application of these copolymers as active layers in photovoltaic cells is also explored.

## 2. Experimental Section

**2.1. Instrumentation.** $^1$H NMR spectra were measured on a Bruker ACF 300 spectrometer with *d*-chloroform as the solvent and tetramethylsilane as the internal reference. UV−visible absorption spectra were measured on a Shimadzu UV 3101PC spectrophotometer using an integrating sphere, ISR-260, the inside of which was coated with a diffusely reflecting material, $BaSO_4$. Elemental microanalysis was performed on a Perkin-Elmer 2400 elemental analyzer. Thermogravimetric analysis (TGA) was conducted on a TA Instruments TGA 2050 thermogravimetric analyzer at a heating rate of 20 °C/min and under a nitrogen flow rate of 100 mL/min. Differential scanning calorimetry (DSC) measurements were carried out on the Mettler Toledo DSC 822$^e$ system under nitrogen and at a heating rate of 10 °C/min. Gel permeation chromatography (GPC) measurements were conducted on a Waters GPC system equipped with a Waters 1515 HPLC pump, Waters Styragel columns, a Water-2487 dual wavelength UV detector, and a Waters 2414 refractive index detector. Polystyrene standards were used as the molecular weight references, and THF was used as the eluent. Cyclic voltammetry (CV) measurement was performed on an Autolab potentiostat/galvanostat system using a three-electrode cell under an argon atmosphere. The polymer film on a Pt disk electrode (working electrode) was scanned (scan rate: 100 mV/s) anodically and cathodically in a 0.1 M acetonitrile solution of tetrabutylammonium hexafluorophosphate ($n$-$Bu_4NPF_6$) with a Ag/AgCl refer-

* To whom correspondence should be addressed. E-mail: cheket@nus.edu.sg (E.-T.K.), klzhang@whu.edu.cn (K.-L.Z.).
† Wuhan University.
‡ Department of Chemical & Biomolecular Engineering, National University of Singapore.
§ Department of Electrical & Computer Engineering, National University of Singapore.

10.1021/ma900236h CCC: $40.75 
Published on Web 03/19/2009

**Scheme 1. Synthesis Route of PTCHO**

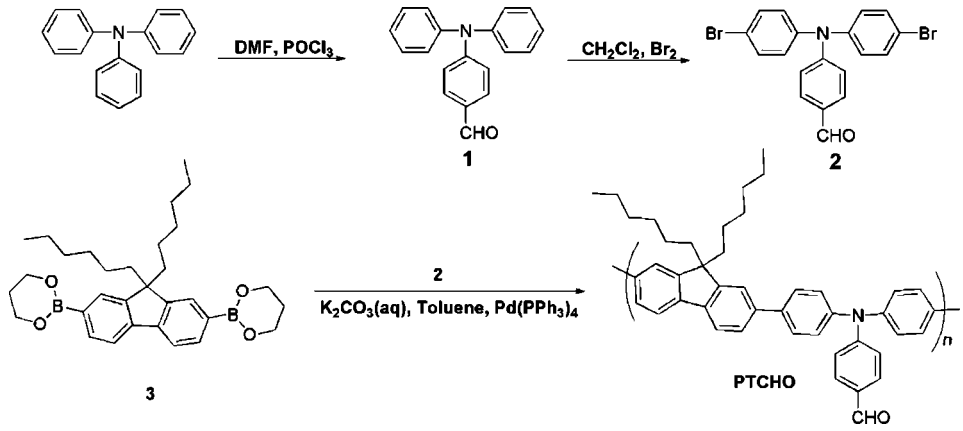


**Scheme 2. Synthesis Routes of PTCN and PTDCN**

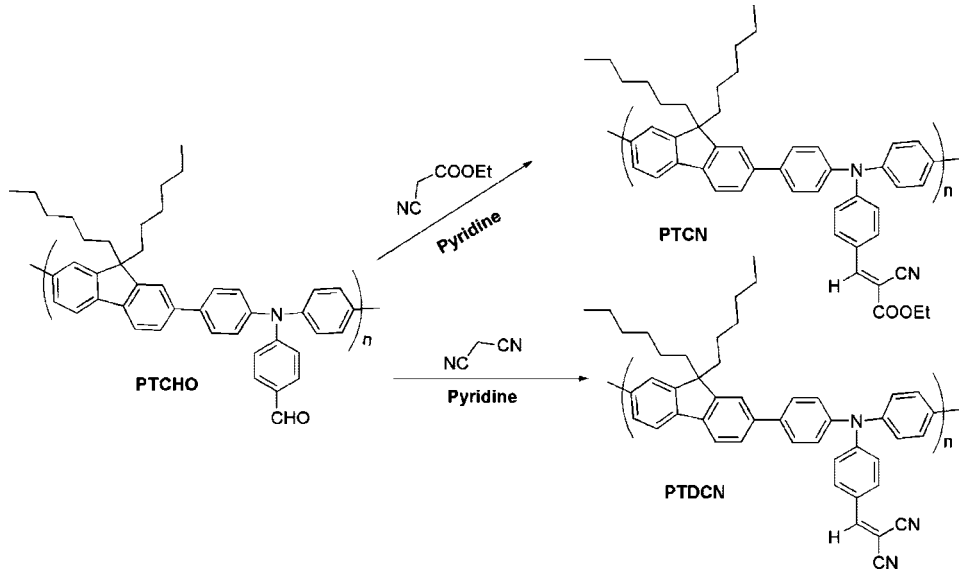


ence electrode and a platinum wire counter electrode. The ferrocene/ferrocenium (Fc/Fc+) couple was used as an internal reference and showed an onset peak at +0.40 eV versus Ag/AgCl. Atomic force microscopic (AFM) images were measured on a nanoscope III A (Digital Instruments) scanning probe microscope using the tapping mode.

**2.2. Photovoltaic Device Fabrication and Characterization.** The indium tin oxide (ITO)-coated glass anodes (20 Ω/sq) were patterned by conventional wet-etching process using concentrated HCl as etchant. After patterning, the substrates were precleaned by sonication sequentially in deionized water, acetone, and isopropanol, followed by oxygen plasma treatment. The hole-collecting layer of poly(3,4-ethylenedioxythiophene)/poly(styrene sulfonate) (PEDOT/PSS, ~40 nm) was spin-coated onto the ITO substrate at 5000 rpm for 30 s, dried in a vacuum oven at 140 °C for 30 min, and then allowed to cool to room temperature in air. The process was followed by spin coating the photoactive layer (~70 nm) from a 20 mg/mL chlorobenzene solution of the copolymer and [6,6]-phenyl-C61-butyric acid methyl ester (PCBM) blend at a component weight ratio of 1:1 or 1:3. After drying in a vacuum oven at 50 °C for 12 h, the aluminum (Al) cathode (200 nm in thickness) was thermally evaporated through a shadow mask to define an active device area of 0.2 $cm^2$. The device was removed from the chamber directly for testing without protective encapsulation. The thickness of the hole-collecting layer and photoactive layer was determined from the edge profile of AFM images. The photocurrent density−voltage ($J-V$) characteristics of the device were measured on a programmable Keithley model 238 electrometer analyzer with AM 1.5G illumination under ambient condition from a Sciencetech solar simulator (model SS150W/SS300W, London, ON Canada) at an intensity of 100 $mW/cm^2$. The mismatch of the simulated spectrum with the solar spectrum was not determined.

**2.3. Materials.** Tetrakis(triphenylphosphine)palladium, or $(PPh_3)_4$-Pd, was prepared according to the method reported in the literature.[31] 9,9-Di-*n*-hexylfluorene-2,7-bis(trimethyleneboronate), trioctylmethylammonium chloride (Aliquat 336), triphenylamine, ethyl cyanoacetate, malononitrile, and solvents (analytical grade) were purchased from Sigma-Aldrich Chemical. The solvents (pyridine, DMF, and toluene) were dried by standard procedures and distilled before use. The synthesis routes for the monomer and the three copolymers are shown in Schemes 1 and 2.

**2.4. 4-(Diphenylamino)benzaldehyde.** The title compound was synthesized according to procedures similar to those reported in the literature.[32] Briefly, 6 mL of dry DMF (77.2 mmol) was added dropwise to 25 mL of phosphorus oxychloride (272 mmol) maintained at 0 °C. After the solution was stirred for 15 min, triphenylamine (**1** in Scheme 1, 5 g, 20.4 mL) was added to the above Vilsmeier reagent,[33] and the mixture was heated to 45 °C for an additional 2 h. After cooling, the clear red solution was added dropwise to ice water with stirring, and the resulting mixture was allowed to stand for 2 h. The crude product was collected by filtration, washed with water, and dissolved in dichloromethane. The organic solution was washed with $H_2O$ (2 × 150 mL) and dried over $MgSO_4$. After the solvent was evaporated off, the residue

was recrystallized from ethyl acetate to afford aldehyde (**2** in Scheme 1) as a pale yellow crystal with a yield of 4.7 g (85%). Melting point: 129−130 °C. $^1$H NMR (300 MHz, $CDCl_3$, $\delta$): 9.80 (s, 1H), 7.67 (d, $J$ = 8.1 Hz, 2H), 7.36−7.25 (m, 4H), 7.28−7.16 (m, 6H), 7.01 (d, $J$ = 8.1 Hz, 2H).

**2.5. 4-(Bis(4-bromophenyl)amino)benzaldehyde.** The title compound was synthesized according the procedure reported in the literature.[15] Bromine (5.9 g, 36.6 mmol) in methylene chloride (50 mL) was added dropwise to 4-(diphenylamino)benzaldehyde (**2**, 5.0 g, 18.3 mmol) in methylene chloride (200 mL) at 0 °C. The mixture was stirred at room temperature for 6 h, and saturated aqueous $Na_2SO_3$ was then added to reduce the remaining bromine. The organic layer was separated, washed with brine (2 × 150 mL), and dried over sodium sulfate. After the solvent was evaporated off, the residue was recrystallized from ethanol to afford a yellow solid with a yield of 6.2 g. Melting point: 157−158 °C. $^1$H NMR (300 MHz, $CDCl_3$, $\delta$): 9.84 (s, 1 H), 7.71 (d, $J$ = 9 Hz, 2H), 7.44 (d, $J$ = 9.0 Hz, 4H), 7.52−7.00 (m, 6H).

**2.6. Poly[2,7-(9,9-dihexylfluorene)-*alt*-1,4-phenylene-4-(formylbenzyl)imino-1,4-phenylene] (PTCHO).** 9,9-Di-*n*-hexylfluorene-2,7-bis(trimethyleneborate) (**3** in Scheme 2, 0.502 g, 1 mmol), 4-(bis(4-bromophenyl)amino)benzaldehyde (**2**, 4.311 g, 1 mmol), Aliquat 336 (20 mg), and $(PPh_3)_4Pd$ (34 mg, 0.03 mmol) (1.5 mol % based on total monomers) were dissolved in degassed toluene (6 mL) in a 25 mL two-necked round-bottomed flask. A 2 M aqueous solution of $K_2CO_3$ (4 mL) was added. The solution was vigorously stirred under argon at 90 °C for 48 h. The resulting mixture was then poured in 200 mL of methanol. The precipitate was collected by filtration and washed with 2 M HCl and methanol. The green solid product was extracted with acetone for 24 h in a Soxhlet apparatus to remove oligomers and catalyst residues.$^1$H NMR (300 MHz, $CDCl_3$, $\delta$): 10.86 (s, 1H), 7.80−7.70 (m, 4H), 7.69 (d, $J$ = 8.4 Hz, 4H), 7.61 (d, $J$ = 8.7 Hz, 4H), 7.33 (d, $J$ = 8.4 Hz, 4H), 7.20 (d, $J$ = 9 Hz, 2H), 7.35−7.18 (m, 6H), 2.36−2.02 (m, 4H), 1.26−1.08 (m, 12H), 0.79−0.74 (m, 10H). Anal. Calcd for $C_{12}H_6N_2O_2$: C, 87.52; H, 7.51; N, 2.32. Found: C, 85.91; H, 7.18; N, 2.28.

**2.7. Poly[2,7-(9,9-dihexylfluorene)-*alt*-2-(4-(diphenylamino)benzylidene)malononitrile] (PTCN).** Ethyl cyanoacetate (10 equiv, 283 mg) was added to a solution of **PTCHO** (150 mg, 0.25 mmol of basic units) in 20 mL of pyridine. The solution turned red immediately and was heated to 55 °C for 48 h. The solution was concentrated under reduced pressure, and the residue was added dropwise to excess methanol to precipitate the polymer as a yellowish-red solid. $^1$H NMR (300 MHz, $CDCl_3$, $\delta$): 8.14 (s, 1H), 7.92 (d, $J$ = 8.7 Hz, 2H), 7.79 (d, $J$ = 7.8 Hz, 2H), 7.69 (d, $J$ = 8.4 Hz, 4H), 7.60 (d, $J$ = 9.6 Hz, 4H), 7.34 (d, $J$ = 8.4 Hz, 4H), 7.16 (d, $J$ = 8.7 Hz, 2H), 4.37 (dd, $J$ = 14.1 Hz, 2H), 2.35−2.01 (m, 4H), 1.39 (t, $J$ = 7.1 Hz, 3H), 1.25−1.08 (m, 12H), 0.78−0.74 (m, 10H). Anal. Calcd for $C_{12}H_6N_2O_2$: C, 84.2; H, 7.21; N, 4.01. Found: C, 83.6; H, 7.50; N, 3.90.

**2.8. Poly[2,7-(9,9-dihexylfluorene)-*alt*-ethyl 3-(4-(diphenylamino)phenyl)-2-cyanoacrylate] (PTDCN).** Malononitrile (10 equiv, 165 mg) was added to a solution of **PTCHO** (150 mg, 0.25 mmol) in 20 mL of pyridine. The solution turned red immediately and was heated to 55 °C for 48 h. The solution was concentrated under reduced pressure, and the residue was added dropwise to excess methanol to precipitate the polymer as a bright-red solid. $^1$H NMR (300 MHz, $CDCl_3$, $\delta$): 7.81 (d, $J$ = 8.1 Hz, 4H), 7.72 (d, $J$ = 8.4 Hz, 4H), 7.61 (d, $J$ = 10.5 Hz, 4H), 7.60 (s, 1H), 7.35 (d, $J$ = 8.4 Hz, 4H), 7.13 (d, $J$ = 8.7 Hz, 2H), 4.37 (dd, $J$ = 14.1 Hz, 2H), 2.35−2.01 (m, 4H), 1.39 (t, $J$ = 7.1 Hz, 3H), 1.25−1.08 (m, 12H), 0.78−0.74 (m, 10H). Anal. Calcd for $C_{12}H_6N_2O_2$: C, 86.60; H, 6.96; N, 6.44. Found: C, 85.93; H, 7.67; N, 6.40.

## 3. Results and Discussion

**3.1. Polymer Synthesis and Characterization.** The synthesis of **PTCHO** was carried out in four steps, as illustrated in Scheme 1. Initially, 4-(diphenylamino) benzaldehyde (**1**) was obtained from triphenylamine via the Vilsmeier reaction[33] with a yield of 79%. Bromination of **1** in methylene chloride at room temperature afforded 4-(bis(4-bromophenyl)amino)benzaldehyde (**2**). The "basic" copolymer, viz. **PTCHO**, was synthesized by Suzuki polycondensation of an equimolecular mixture of the dibromide and diboronate (**3**). The copolymerization was carried out for 48 h using $Pd(PPh_3)_4$ as the catalyst in a two-phase mixture of degassed toluene and aqueous $K_2CO_3$ (2.0 M) and in the presence of Aliquat 336 as a phase transfer reagent.

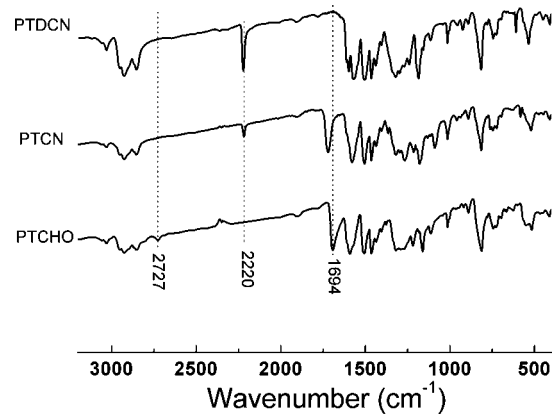


**Figure 1.** FT-IR spectra of the copolymers.

Molecular weight of conjugated polymers is one of the key parameters governing their physicochemical and electronic properties, such as mobility of charge carriers, processability, and film morphology, in bulk-heterojunction solar cells, field effect transistors, and light emitting diodes.[13,34,35] Therefore, polymers with similar molecular architecture and bearing a comparable number of conjugation units are more desirable for the study of the structure−property relationship. However, the number of conjugation units along the backbone usually cannot be precisely controlled because of the nature of polymerization reactions and different reactivity of monomers. This problem can be overcome by modifying the pendant groups of a conjugated polymer, such as **PTCHO**, to form **PTCN** and **PTDCN** (Scheme 2).

As shown in Scheme 2, **PTCHO** was condensed with ethyl cyanoacetate and malononitrile to afford **PTCN** and **PTDCN**, respectively. The optimum reaction conditions for achieving complete conversion of the aldehyde groups were found to be in pyridine at 55 °C for 48 h. The presence of triethylamine or piperidine as a base did not improve the conversion efficiency of the aldehyde groups in methylene chloride or chloroform and generally resulted in undesirable byproduct. After purifications and drying, **PTCHO**, **PTCN**, and **PTDCN** were obtained as green, yellowish-red, and bright-red solids, respectively, indicating significant differences in their effective conjugation lengths. The conversion of aromatic aldehyde of **PTCHO** was revealed by Fourier transform infrared (FT-IR) absorption spectroscopy. As shown in Figure 1, the characteristic absorption peaks of the −CHO group appear at 1694 and 2724 $cm^{-1}$, associated with the C−H and C═O stretching vibrations, respectively.[36] After modification, these characteristic absorptions of aldehyde have disappeared. New absorption peaks at 2217 $cm^{-1}$ (for **PTCN** and **PTDCN**) and 1710 $cm^{-1}$ (for **PTCN**), corresponding, respectively, to C≡N stretching vibration of the nitrile group and C═O stretching vibration of the carboxylic ester, have emerged, which is indicative of nearly complete conversion of the terminal aldehyde group. The chemical structures of the copolymers were also verified by $^1$H NMR spectroscopy. The assignments of chemical shifts in the $^1$H NMR spectra are shown in Figure 2. The complete disappearances of the aldehyde proton signal at 9.8 ppm and the appearances of olefinic proton signals at 8.14 ppm[37] for **PTCN** and 7.56 ppm for **PTDCN** provide confirmation of the

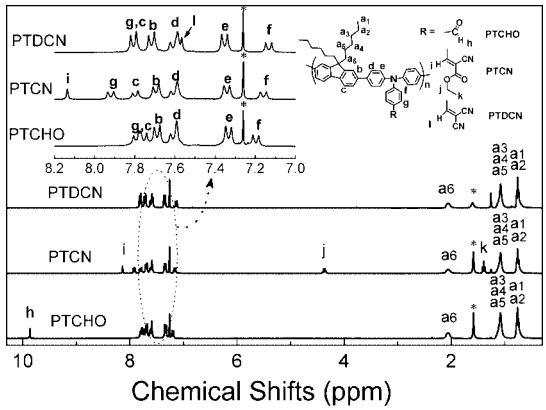


**Figure 2.** $^1$H NMR spectra of the synthesized copolymers in $CDCl_3$, with the solvent peaks marked by asterisks (*). The inset shows the expanded view in the low fields.

**Table 1. Molecular Weights[a] and Thermal Properties of the Donor−Acceptor Alternating Conjugated Copolymers**

| polymers | $M_w$ | $M_n$ | PDI ($M_w/M_n$) | DSC (°C)[b] | $T_d$ (°C)[c] |
|---|---|---|---|---|---|
| PTCHO | 20 382 | 50 160 | 2.46 | 195 | 425 |
| PTCN | 24 680 | 55 982 | 2.26 | 183 | 372 |
| PTDCN | 22 883 | 54 744 | 2.39 | 184 | 394 |

[a] Molecular weights and polydispersity indexes were determined by GPC in THF using polystyrene as standards. [b] 5% weight loss temperature measured by TGA under $N_2$. [c] Glass-transition temperature measured by DSC under $N_2$.

**Table 2. Physical Properties of the Donor−Acceptor Alternating Conjugated Copolymer Films**

| polymers | $\lambda_{abs}$ (nm)[a] | $\lambda_{em}$ (nm)[a] | $E_g$ (eV)[b] | $E_{ox}$ (eV)[c] | HOMO (eV)[d] | LUMO (eV)[e] |
|---|---|---|---|---|---|---|
| PTCHO | 376 | 489 | 2.96 | 1.10 | −5.50 | −2.74 |
| PTCN | 371, 442 | 576 | 2.46 | 1.12 | −5.51 | −3.20 |
| PTDCN | 364, 464 | 627 | 2.39 | 1.14 | −5.54 | −3.36 |

[a] Obtained from thin films. [b] Band gap, estimated from the optical absorption band edge of the films. [c] Calculated from the onset oxidation potentials. [d] Estimated using empirical equations $E_{HOMO} = [(E_{ox} - E_{Foc}) + 4.8]$. [e] Estimated using empirical equations $E_{LUMO} = E_{HOMO} - E_g$.

efficient conversion reaction. In addition, the ratios of integrated peak areas of olefinic to aliphatic protons and of olefinic to aromatic protons are consistent with the proposed structures of **PTCN** and **PTDCN**, as depicted in Scheme 2.

As determined by gel permeation chromatography (GPC), **PTCHO** has a number-average molecular weight ($M_n$) of 5.02 × $10^4$, corresponding to a degree of polymerization of about 34, with a polydispersity index of 2.46. The modification has led to a slight increase in the molecular weights of the resulting copolymers, as shown in Table 1. The $M_n$ values of **PTCN** and **PTDCN** were found to be 5.60 × $10^4$ and 5.47 × $10^4$, respectively, with the corresponding polydispersity indices of 2.26 and 2.39. All three copolymers are readily soluble in common organic solvents, such as tetrahydrofuran, toluene, chloroform, and chlorobenzene and can be readily cast into uniform thin films, rendering them good candidates for the fabrication of organic semiconductors.

**3.2. Thermal Stability.** The thermal properties of the copolymers were determined via thermogravimetric analysis (TGA) and differential scanning calorimetry (DSC) under a nitrogen atmosphere. As shown in Table 2, the 5% weight-loss temperatures for **PTCHO**, **PTCN**, and **PTDCN** are in the range of 372−425 °C. The copolymers have glass-transition temperatures ($T_g$) ranging from 183 to 195 °C. Such high values of $T_g$, which can retard morphological changes and suppress formation of aggregates at elevated temperatures, are desirable for polymers to be used as electroactive materials in organic semiconductor applications.[38]

**3.3. Optical Properties.** To assess their photophysical properties, we measured the absorption and PL spectra of **PTCHO**, **PTCN**, and **PTDCN** in solution and in the film form (Figure 3). The toluene solution of **PTCHO** has an absorption maximum at 378 nm (Figure 3a) corresponding to the $\pi$-$\pi$* transition of the polymer backbone and blue-shifted by ∼10 nm relative to that of the fluorene-*alt*-triphenylamine copolymers.[29] The spectral shift can probably be attributed to distortion of the backbone, thereby reducing the effective conjugation length, arising from orbital interactions between the aromatic aldehyde and triphenylamine group. Differing from **PTCHO** and in addition to the absorption of fluorene-*alt*-triphenylamine backbones at ∼372 nm, the introduction of electron-withdrawing pendant groups produces new absorption bands at 440 nm for **PTCN** and 452 nm for **PTDCN**, attributable to intramolecular charge transfer (ICT) interactions[39] between the polymer backbone and the pendant acceptor groups. Evidently, the ICT interaction is more significant for the dicyano-substituted polymer (**PTDCN**) than for the monocyano-substituted polymer (**PTCN**) because of the increased $\pi$-conjugation and enhanced electron-accepting ability of the dicyano moiety. For the as-spun film on glass substrates, the UV−visible absorption spectra of the three copolymers are red-shifted and broadened (Figure 3b), as compared with the corresponding dilute solution spectra. The red-shift and broadening of the solid-state absorption spectra are probably related to the increased extent of $\pi$-$\pi$ stacking alignment of the backbones, increased polarizability of the film, or both.[40,41]

In both solutions and the film form, the $\pi$-$\pi$* transitions of the backbones are progressively blue-shifted when the pendant acceptor groups are varied from the aldehyde group to the monocyano group and further to the dicyano group. This phenomenon is probably also related to the increasing extent of distortion of the backbones, similar to that of **PTCHO** relative to the unsubstituted fluorene-triphenylamine copolymer, as discussed above. Furthermore, the conformational distortion of the backbone is related to the nature of the acceptor groups, as suggested by theoretical calculations (see below).

The three copolymers exhibit different emission colors in solution upon excitation at the wavelength of 380 nm, as shown in Figure 3c. The emission spectra of **PTCHO**, **PTCN**, and **PTDCN** have maxima at 468, 550, and 575 nm, respectively, approximately corresponding to blue, yellowish-green, and yellowish-orange emissions. Similar to their absorption spectra, this difference in emission wavelengths among the three copolymers can be understood in terms of the strength of the donor−acceptor interaction, which can affect the excited states.

The solid-state PL spectrum of the three copolymers is red-shifted by about 20, 28, and 50 nm, respectively, from the corresponding solution spectra (Figure 3d). This phenomenon is probably attributable to intermolecular interactions, leading to aggregation and possible excimer formation.[42,43] Therefore, blue, yellowish-green, and yellowish-orange fluorescence are observed for the as-spun films of **PTCH**, **PTCN**, and **PFDCN**, respectively, when irradiated at the wavelength of 365 nm (Figure 4). The variation in emission wavelengths of **PTCHO**, **PTCN**, and **PTDCN** suggests the possibility of tuning the photophysical properties of fluorene-*alt*-triphenylamine conjugated copolymers for full-color-display applications by the simple manipulation of acceptor strength in the pendant groups.

**3.4. Electrochemical Properties and Energy Levels.** The highest occupied molecular orbital (HOMO) and the lowest unoccupied molecular orbital (LUMO) energy levels of the conjugated polymers are important parameters in the design of semiconductor and junction devices. The voltammograms and

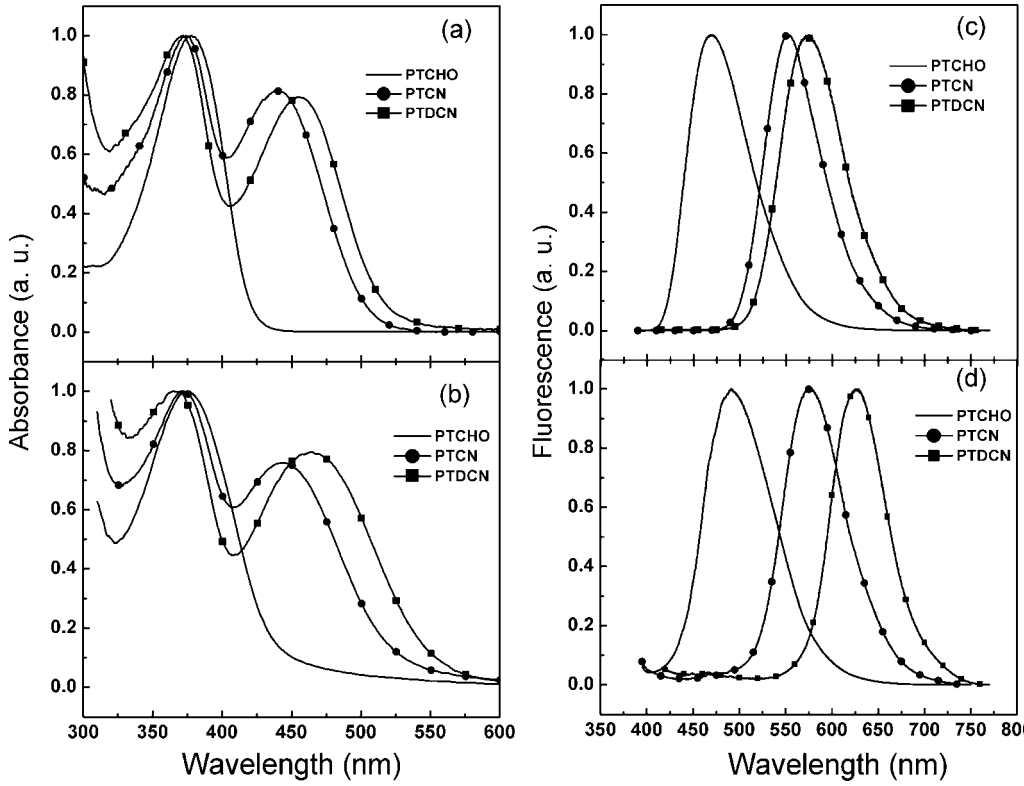


**Figure 3.** UV−visible absorption spectra of the polymers (a) in toluene solution and (b) in the film form. Fluorescence spectra of the copolymers (c) in toluene solution and (d) in the film form ($\lambda_{ex}$ = 380 nm).

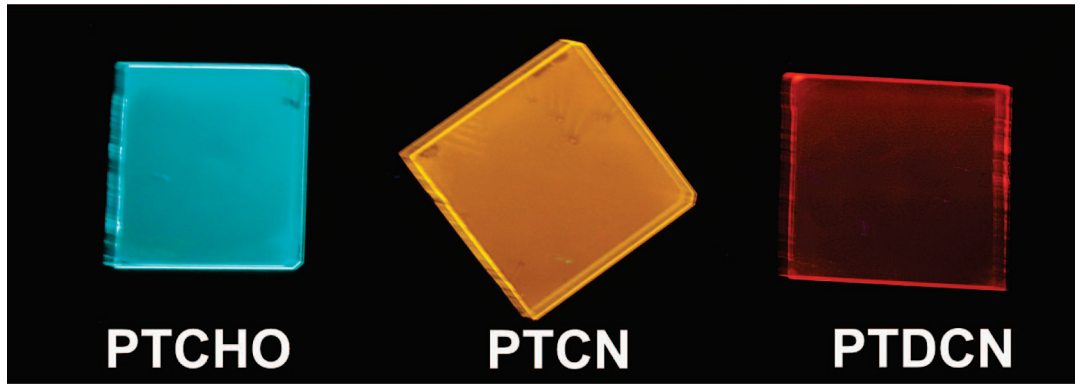


**Figure 4.** Fluorescence of the spun films of PTCHO, PTCN, and PTDCN under UV irradiation ($\lambda_{ex}$ = 365 nm).

the onset oxidation potentials ($E_{ox}$) of the three copolymers are shown in Figure 5 and Table 2, respectively. There were two oxidation peaks, the first reversible one corresponds to the oxidation of the triphenylamine moiety, and the second corresponds to the oxidation of the fluorene ring. Therefore, the HOMO energy values of the polymers were estimated according to that (−4.8 eV) of ferrocene (Fc) with respect to the vacuum level.[44] Because the reduction curves could hardly be obtained, the optical absorption band edge of the film was utilized to derive the band gap and calculate the LUMO energy levels of each copolymer. As shown in Table 2, the HOMO and LUMO energy levels of **PTCHO** are −5.50 and −2.74 eV, respectively. After modification, the HOMO energy levels of **PTCN** and **PTDCN** remain unchanged despite the presence of different pendant acceptor groups, whereas their LUMO energy levels have decreased.

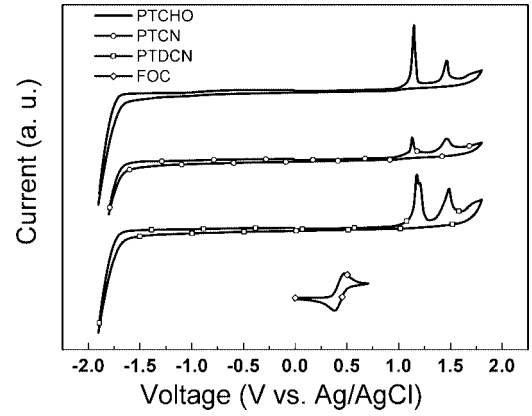


**Figure 5.** Cyclic voltammograms of the copolymers in acetonitrile at a sweep rate of 100 mV/s.

**3.5. Theoretical Calculations.** To provide further insight into the fundamentals of molecular architecture, molecular simulation was carried out for **PTCHO**, **PTCN**, and **PTDCN** with a chain length of $n$ = 2 at the DFT B3LYP/6-31G(d) level with the Gaussian 03 program package.[45] The hexyl groups of the fluorine unit were not included in the calculation to avoid

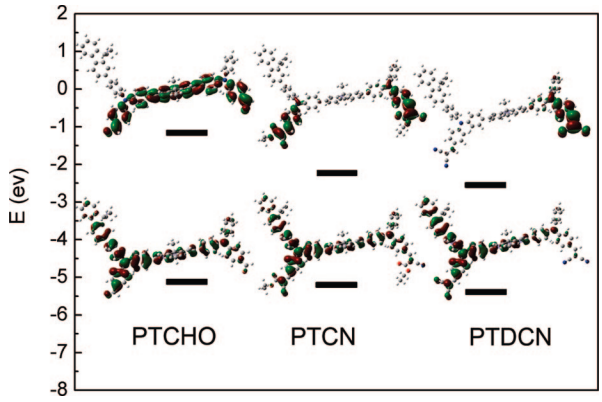


**Figure 6.** HOMO and LUMO energy levels (eV) and the frontier molecular orbitals obtained from DFT calculations on PTCHO, PTCN, and PTDCN with a chain length $n = 2$ at B3LYP/6-31G* level.

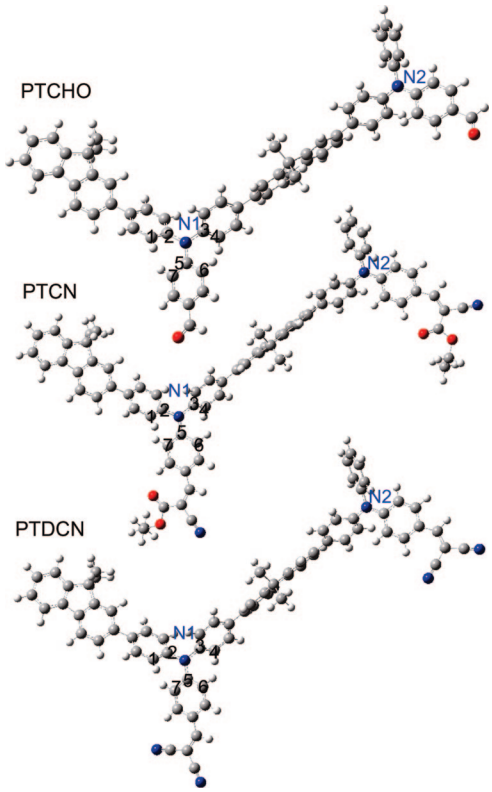


**Figure 7.** Optimized geometry of PTCHO, PTCN, and PTDCN with a chain length of $n = 2$ at the B3LYP/6-31G* level of theory.

excessive computation demand because they do not significantly affect the equilibrium geometry and thus the electronic properties. As depicted in Figure 6, the LUMOs for all of the polymers are located on the peripheral triphenylamine groups and on the adjacent fluorene rings. As a result, the computed HOMOs are close to one another. For **PTCHO**, there is a significant overlap between the HOMO and LUMO. However, the electron density distributions at LUMO become highly localized near the electron-withdrawing cyano groups for **PTCN** and **PTDCN**, and the well-separated distribution of HOMO and LUMO levels indicate that a transition between them can be considered to be a charge-transfer transition.

The optimized geometries are shown in Figure 7, and the relevant geometrical parameters are listed in Table 3. The structural differences in the amine groups of **PTCHO**, **PTCN**, and **PTDCN** are described by two parameters: (i) the C−N bond length and (ii) the dihedral angle between the *N*-phenyl planes (one located on the backbone and one bearing the pendant acceptor group). Larger orbital overlaps among the amine nitrogen moieties can be expected if the C−N bond lengths are more evenly distributed and the dihedral value is close to 0°. The data in Table 3 are derived from the N1 moiety. Those from the N2 moiety show results similar to those described below. First of all, the substituent effects were reflected on the C−N1 bond lengths of the triphenylamine moiety. As shown in Table 3, when the substituent group is changed from aldehyde to monocyano and then to dicyano group, the C5−N1 bond lengths for **PTCHO**, **PTCN**, and **PTDCN** are progressively shortened, whereas the bond lengths of C2−N1 and C3−N1 progressively increase. However, the C1−C2−N1-C5 dihedral angles of 45.7, 47.1, and 48.6, along with the C3−C4−N1−C5 dihedral angels of 48.2, 49.5, and 60.0, respectively, for **PTCHO**, **PTCN**, and **PTDCN**, were recorded. The progressive increase in the dihedral angle and uneven distribution of the C−N bond length are associated with the degree of distortion of the triphenylamine groups induced by the pendant acceptor groups. This effect increases in the order aldehyde group < monocyano group < dicyano group. The calculation results indicate that the stronger the attached pendant acceptor group, the poorer the effective conjugation of the backbone. Therefore, the calculation results are in good agreement with the observed blue shift of the $\pi$-$\pi^*$ transitions of the backbone of the copolymers in both solution and the solid state.

Upon irradiation in the solid state, the unique electron distribution patterns of **PTCN** and **PTDCN** will facilitate the recombination of excited molecules with the nearby ground-state molecules by intermolecular charge transfer interactions between the cyano groups and the fluorene−triphenylamine donors, resulting in the formation of excimers.[46,47] Therefore, in addition to molecular aggregation, the excimer formation can also contribute to the observed red shift in emission.

In addition, it can be seen from Figure 6 and Table 2 that although discrepancies exist between the calculation and experimental results, the trends of variation in the HOMO and LUMO energies, as well as the energy gaps, are similar. The presence of pendant cyano groups with strong electron affinity leads to a decrease in the LUMO energies but affects the HOMO levels to a much lesser extent. The similarity in HOMO levels suggests that electron coupling between the alternating triphenylamine−fluorene backbone and the different electron acceptor groups does not affect hole generation in the bulk of the resultant polymer to a significant extent, as is evident from the cyclic voltammetry measurements.

**3.6. Photovoltaic Properties.** Two molecular architectures have been commonly adopted for turning the energy levels in donor−acceptor conjugated polymers. One involves alternating donor—acceptor units in the main chains, and the other comprises pendant acceptor groups and donor main chains. The latter architecture has the advantage of allowing charge separation through sequential transfer of electrons from the main chains to the side chains and then to [6,6]-phenyl-C61-butyric acid methyl ester (PCBM)[48] in a heterojunction device. Accordingly, the potential application of these copolymers as active layers in photovoltaic cells was investigated.

Because the absorption spectra of **PTCN** and **PTDCN** can provide a better overlap with the solar spectrum than **PTCHO**, only the photovoltaic characteristics of **PTCN** and **PTDCN** were studied. Bulk heterojunction solar cells based on **PTCN** and **PTDCN**, in combination with the well-known fullerene acceptor (PCBM) at a weight ratio of 1:1 and 1:3, were prepared. Performance characteristic of the photovoltaic cells are summarized in Table 4.

The weight ratio of the copolymer to PCBM has a significant effect on the performance of the cell. As shown in Table 4, a 1:1 weight ratio of copolymer/PCBM gives better performance

**Table 3. Relevant Bond Distances, Bond Angles, and Torsional Angles of the Optimized Geometries for the Polymers**

| | C−N bond distance (Å)[a] | dihedral angles (deg)[a] | CNC bond angle (deg)[a] | |
|---|---|---|---|---|
| | C2−N1, C3−N1, C5−N1 | C1−C2−N1−C5, C3−C4−N1−C5 | C2N1C3, C2N1C3, C2N1C3 | dipole moment (debye)[b] |
| PTCHO | 1.425, 1.426, 1.407 | 45.7, 48.1 | 118.0, 120.9, 121.1 | 8.93 |
| PTCN | 1.427, 1.428, 1.401 | 47.4, 49.5 | 118.2, 120.8, 121.0 | 12.42 |
| PTDCN | 1.429, 1.429, 1.397 | 48.6, 60.0 | 118.6, 120.6, 120.8 | 18.28 |

[a] Derived from the N1 moiety. [b] Derived from the entire unit.

**Table 4. Characteristic Current Density−Voltage Parameters from Devices Tested under Standard AM 1.5G Conditions**

| polymer/PCBM (w/w ratio) | | $J_{sc}$ (mA/cm$^2$) | $V_{oc}$ (V) | FF | PCE (%) |
|---|---|---|---|---|---|
| PTCN | 1:1 | 1.06 | 0.85 | 0.24 | 0.22 |
| | 1:3 | 0.85 | 0.62 | 0.16 | 0.08 |
| PTDCN | 1:1 | 0.61 | 0.87 | 0.20 | 0.11 |
| | 1:3 | 0.36 | 0.74 | 0.18 | 0.05 |

in the present photovoltaic systems. Under 1.5G illumination (100 mW/cm$^2$), the cell based on **PTDCN**/PCBM as the active layer has a short circuit current density ($J_{SC}$) of 0.61 mA/cm$^2$, an open circuit voltage ($V_{OC}$) of 0.87 V, a calculated fill factor (FF) of 0.20, and power conversion efficiency (PCE) of 0.11%, as shown in Figure 8. Enhanced solar cell performance was obtained for the device based on **PTCN**/PCBM, 1.06 mA/cm$^2$ ($J_{SC}$), 0.85 V ($V_{OC}$), 0.24 (FF), and 0.22% (PCE). A further increase in the PCBM content (1:3 weight ratio of copolymer/PCBM) resulted in a decrease in $J_{SC}$ and PCE, probably because of the reduction in concentration of the photoactive polymer and poorer intermolecular packing of the donor polymers, which in turn resulted in reduced absorption[49] and carrier transport in the donor domains,[50] respectively.

The power conversion efficiency obtained for devices based on **PTCN** is considerably higher than that for devices based on **PTDCN**, despite the poorer mismatch between absorption spectra of the former and the solar irradiance spectrum. To clarify this phenomenon, the morphology of the composite films was studied by atomic force microscopy (AFM). Figure 9a shows a typical AFM image and the topographical roughness of a 1:3 weight ratio of the **PTCN**/PCBM composite film. A high degree of homogeneity is observed for the film. In contrast, the corresponding **PTDCN**/PCBM composite film exhibits substantial phase segregation and high surface roughness (Figure 9b), suggesting poor dispersion of PCBM in the copolymer matrix. Similar morphology was observed for the **PTDCN**/PCBM composite film of 1:1 weight ratio. It has been recently reported that chemical similarity between the functional groups attached to the donor polymer and the fullerene leads to the

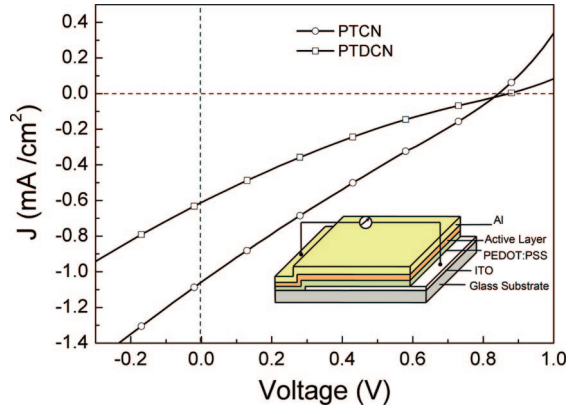


**Figure 8.** Current density−voltage characteristics of bulk-heterojunction solar cells of the 1:1 weight ratio composite films of PTCN/PCBM and PTDCN/PCBM. The inset shows the schematic diagram of the device.

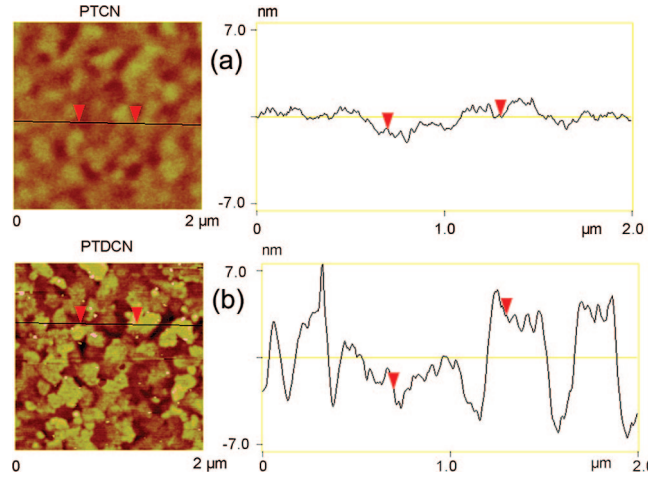


**Figure 9.** Tapping mode AFM topography images (2 × 2 $\mu$m$^2$) of the 1:3 (weight ratio) composite films of (a) PTCN/PCBM and (b) PTDCN/PCBM and the corresponding topographical roughness.

formation of films with uniform and stable nanophase morphologies.[51] In the present case, the significant morphological difference between the two composite polymer films suggests that chemical similarity of the carboxylic ester functionality attached to **PTCN** and PCBM can improve the miscibility between them in the composite film, thereby efficiently suppressing the tendency of the PCBM molecules to phase segregate into microscale clusters. Aggregation of the PCBM molecules is thought to decrease the charge carrier mobility for electrons because separations among the clusters can result in large barriers to the hopping process, [52] accounting for the poor performance of the **PTDCN** devices.

Because the hybrid systems of donor−acceptor dyads bearing triphenylamine core and terminal cyano group have demonstrated prominent photovoltaic effects,[53−55] attempts to optimize the solar cell structure (such as bilayer cells, film thickness, electrode materials) or processing conditions (such as annealing temperature) as well as work on the modification of polymer structure to extend the absorption spectrum of the donor polymers into longer wavelengths are ongoing.

## 4. Conclusions

Three triphenylamine−fluorene alternating conjugated copolymers bearing respective aldehyde, monocyano, and dicyano pendant acceptor groups have been successfully synthesized. **PTCHO** with the aldehyde pendant groups was synthesized via the Suzuki coupling method, whereas **PTCN** with monocyano and **PTDCN** with dicyano pendant groups were synthesized via chemical modification of **PTCHO**. Because of the high reactivity of the aldehyde groups and optimized reaction conditions, the conversion of the aldehyde groups was efficient, as verified by $^1$H NMR and FT-IR spectroscopies. The synthesis strategy has allowed the direct comparison of polymers with the same number of conjugation units for elucidating their structure−property relationships. The obtained copolymers exhibit excellent solubility in common organic solvents and good thermal stability. Through manipulating the strength of the acceptor groups attached to the $\pi$-conjugated copolymer backbone, the energy

levels, and thus the photophysical and electronic properties of the copolymers, can be effectively tuned, for example, to produce nearly primary color emissions. The chemical modification approach thus provides a simple and effective means for tuning the emission in conjugated polymers for full-color or white-light display, as well as for the rational design of electroactive polymers for photoelectronic applications. **PTCN** and **PTDCN** were successfully incorporated as active layers in photovoltaic cells. Moderate device performance, with PCE of 0.11% and $V_{oc}$ of 0.87 V, was obtained for the device with a **PTDCN**/PCBM ratio of 1:1, whereas for the device with a **PTCN**/PCBM ratio of 1:1, PCE up to 0.22% and $V_{oc}$ of 0.85 V were obtained.

## References and Notes


(1) Liu, J. Y.; Zhang, R.; Sauve, G.; Kowalewski, T.; McCullough, R. D. *J. Am. Chem. Soc.* **2008**, *130*, 13167–13176.
(2) Kulkarni, A. P.; Tonzola, C. J.; Babel, A.; Jenekhe, S. A. *Chem. Mater.* **2004**, *16*, 4556–4573.
(3) Shu, C. F.; Dodda, R.; Wu, F. I.; Liu, M. S.; Jen, A. K. Y. *Macromolecules* **2003**, *36*, 6698–6703.
(4) Thompson, B. C.; Frechet, J. M. J. *Angew. Chem, Int. Ed.* **2008**, *47*, 58–77.
(5) Witker, D.; Reynolds, J. R. *Macromolecules* **2005**, *38*, 7636–7644.
(6) Zhang, K.; Tieke, B. *Macromolecules* **2008**, *41*, 7287–7295.
(7) Tsami, A.; Yang, X.; Farrell, T.; Neher, D.; Holder, E. *J. Polym. Sci., Part A: Polym. Chem.* **2008**, *46*, 7794–7808.
(8) Durben, S.; Nickel, D.; Krüger, R.; Baumgartner, T. *J. Polym. Sci., Part A: Polym. Chem.* **2008**, *46*, 8179–8190.
(9) Yasuda, T.; Namekawa, K.; Iijima, T.; Yamamoto, T. *Polymer* **2007**, *48*, 4375–4384.
(10) Liu, C.-L.; Tsai, J.-H.; Lee, W.-Y.; Chen, W.-C.; Jenekhe, S. A. *Macromolecules* **2008**, *41*, 6952–6959.
(11) Wettach, H.; Pasker, F.; Höger, S. *Macromolecules* **2008**, *41*, 9513–9515.
(12) Yu, W. L.; Meng, H.; Pei, J.; Huang, W. *J. Am. Chem. Soc.* **1998**, *120*, 11808–11809.
(13) Huang, B.; Li, J.; Jiang, Z.; Qin, J.; Yu, G.; Liu, Y. *Macromolecules* **2005**, *38*, 6915–6922.
(14) Chan, L.-H.; Lee, Y.-D.; Chen, C.-T. *Macromolecules* **2006**, *39*, 3262–3269.
(15) Lee, S. K.; Hwang, D. H.; Jung, B. J.; Cho, N. S.; Lee, J.; Lee, J. D.; Shim, H. K. *Adv. Funct. Mater.* **2005**, *15*, 1647–1655.
(16) Zhu, Z.; Waller, D.; Gaudiana, R.; Morana, M.; Muhlbacher, D.; Scharber, M.; Brabec, C. *Macromolecules* **2007**, *40*, 1981–1986.
(17) Galand, E. M.; Kim, Y. G.; Mwaura, J. K.; Jones, A. G.; McCarley, T. D.; Shrotriya, V.; Yang, Y.; Reynolds, J. R. *Macromolecules* **2006**, *39*, 9132–9142.
(18) Li, Y. F.; Zou, Y. P. *Adv. Mater.* **2008**, *20*, 2952–2958.
(19) Bundgaard, E.; Krebs, F. C. *Sol. Energy Mater. Sol. Cells* **2007**, *91*, 954–985.
(20) Zhu, Y.; Champion, R. D.; Jenekhe, S. A. *Macromolecules* **2006**, *39*, 8712–8719.
(21) Yamamoto, T.; Yasuda, T.; Sakai, Y.; Aramaki, S.; Ramaw, A. *Macromol. Rapid Commun.* **2005**, *26*, 1214–1217.
(22) Yamamoto, T.; Kokubo, H.; Kobashi, M.; Sakai, Y. *Chem. Mater.* **2004**, *16*, 4616–4618.
(23) Ling, Q. D.; Song, Y.; Lim, S. L.; Teo, E. Y. H.; Tan, Y. P.; Zhu, C. X.; Chan, D. S. H.; Kwong, D. L.; Kang, E. T.; Neoh, K. G. *Angew. Chem., Int. Ed.* **2006**, *45*, 2947–2951.
(24) Ling, Q. D.; Chang, F. C.; Song, Y.; Zhu, C. X.; Liaw, D. J.; Chan, D. S. H.; Kang, E. T.; Neoh, K. G. *J. Am. Chem. Soc.* **2006**, *128*, 8732–8733.
(25) Morteani, A. C.; Dhoot, A. S.; Kim, J. S.; Silva, C.; Greenham, N. C.; Murphy, C.; Moons, E.; Cina, S.; Burroughes, J. H.; Friend, R. H. *Adv. Mater.* **2003**, *15*, 1708–1712.
(26) Bodrozic, V.; Brown, T. M.; Mian, S.; Caruana, D.; Roberts, M.; Phillips, N.; Halls, J. J.; Grizzi, I.; Burroughes, J. H.; Cacialli, F. *Adv. Mater.* **2008**, *20*, 2410–2415.
(27) Yim, K. H.; Whiting, G. L.; Murphy, C. E.; Halls, J. J. M.; Burroughes, J. H.; Friend, R. H.; Kim, J. S. *Adv. Mater.* **2008**, *20*, 3319–3324.
(28) Nilsson, S.; Bernasik, A.; Budkowski, A.; Moons, E. *Macromolecules* **2007**, *40*, 8291–8301.
(29) Kim, J. S.; Lu, L.; Sreearunothai, P.; Seeley, A.; Yim, K. H.; Petrozza, A.; Murphy, C. E.; Beljonne, D.; Cornil, J.; Friend, R. H. *J. Am. Chem. Soc.* **2008**, *130*, 13120–13131.
(30) Westenhoff, S.; Howard, I. A.; Hodgkiss, J. M.; Kirov, K. R.; Bronstein, H. A.; Williams, C. K.; Greenham, N. C.; Friend, R. H. *J. Am. Chem. Soc.* **2008**, *130*, 13653–13658.
(31) Coulson, D. R. *Inorganic Syntheses*; McGraw Hill: New York, 1972; Vol. *XIII*.
(32) Lee, T. H.; Tong, K. L.; So, S. K.; Leung, L. A. *Synth. Met.* **2005**, *155*, 116–124.
(33) Laue, T.; Plagens, A. Ch. 19. In *Named Organic Reactions*, 2nd ed.; John Wiley & Sons: Hoboken, NJ, 2005; pp 280−284.
(34) Pokrop, R.; Verilhac, J. M.; Gasior, A.; Wielgus, I.; Zagorska, M.; Travers, J. P.; Pron, A. *J. Mater. Chem.* **2006**, *16*, 3099–3106.
(35) Demadrille, R.; Delbosc, N.; Kervella, Y.; Firon, M.; De Bettignies, R.; Billon, M.; Rannou, P.; Pron, A. *J. Mater. Chem.* **2007**, *17*, 4661–4669.
(36) Fang, Q.; Yamamoto, T. *Macromolecules* **2004**, *37*, 5894–5899.
(37) Meng, F. S.; Liu, C. Z.; Hua, J. L.; Cao, Y.; Chen, K. C.; Tian, H. *Eur. Polym. J.* **2003**, *39*, 1325–1331.
(38) Li, J. Y.; Liu, D.; Li, Y. Q.; Lee, C. S.; Kwong, H. L.; Lee, S. T. *Chem. Mater.* **2005**, *17*, 1208–1212.
(39) Leriche, P.; Frere, P.; Cravino, A.; Aleveque, O.; Roncali, J. *J. Org. Chem.* **2007**, *72*, 8332–8336.
(40) Shang, Y. L.; Wen, Y. Q.; Li, S. L.; Du, S. X.; He, X. B.; Cai, L.; Li, Y. F.; Yang, L. M.; Gao, H. J.; Song, Y. *J. Am. Chem. Soc.* **2007**, *129*, 11674–11675.
(41) Surin, M.; Sonar, P.; Grimsdale, A. C.; Mullen, K.; De Feyter, S.; Habuchi, S.; Sarzi, S.; Braeken, E.; Heyen, A. V.; Van der Auweraer, M.; De Schryver, F. C.; Cavallini, M.; Moulin, J. F.; Biscarini, F.; Femoni, C.; Roberto, L.; Leclere, P. *J. Mater. Chem.* **2007**, *17*, 728–735.
(42) Jenekhe, S. A.; Osaheni, J. A. *Science* **1994**, *265*, 765–768.
(43) Teetsov, J.; Fox, M. A. *J. Mater. Chem.* **1999**, *9*, 2117–2122.
(44) Lee, Y. Z.; Chen, X.; Chen, S. A.; Wei, P. K.; Fann, W. S. *J. Am. Chem. Soc.* **2001**, *123*, 2296–2307.
(45) Frisch, M. J.; Trucks, G. W., Schlegel, H. B., Scuseria, G. E., Robb, M. A.; Cheeseman, J. R.; Montgomery, J. A., Jr.; Vreven, T.; Kudin, K. N.; Burant, J. C.; Millam, J. M.; Iyengar, S. S.; Tomasi, J.; Barone, V.; Mennucci, B.; Cossi, M.; Scalmani, G.; Rega, N.; Petersson, G. A.; Nakatsuji, H.; Hada; M.; Ehara; M.; Toyota, K.; Fukuda, R.; Hasegawa, J.; Ishida, M.; Nakajima, T.; Honda, Y.; Kitao, O.; Nakai, H.; Klene, M.; Li, X.; Knox, J. E.; Hratchian, H. P.; Cross, J. B.; Bakken, V.; Adamo, C.; Jaramillo, J.; Gomperts, R.; Stratmann, R. E.; Yazyev, O.; Austin, A. J.; Cammi, R.; Pomelli, C.; Ochterski, J. W.; Ayala, P. Y.; Morokuma, K.; Voth; G. A.; Salvador, P.; Dannenberg, J. J.; Zakrzewski, V. G.; Dapprich, S.; Daniels, A. D.; Strain, M. C.; Farkas, O.; Malick, D. K.; Rabuck, A. D.; Raghavachari, K.; Foresman, J. B.; Ortiz, J. V.; Cui, Q.; Baboul, A. G.; Clifford, S.; Cioslowski, J.; Stefanov, B. B.; Liu, G.; Liashenko, A.; Piskorz, P.; Komaromi, I.; Martin, R. L.; Fox, D. J.; Keith, T.; Al-Laham, M. A.; Peng, C. Y.; Nanayakkara, A.; Challacombe, M.; Gill, P. M. W.; Johnson, B.; Chen, W.; Wong, M. W.; Gonzalez, C.; Pople, J. A. *Gaussian 03*, revision C.02; Gaussian, Inc.: Wallingford, CT, 2004.
(46) Liu, Y.; Tao, X. T.; Wang, F. Z.; Dang, X. N.; Zou, D. C.; Ren, Y.; Jiang, M. H. *J. Phys. Chem. C* **2008**, *112*, 3975–3981.
(47) Jiang, X.; Yang, X. C.; Zhao, C. Z.; Jin, K.; Sun, L. C. *J. Phys. Chem. C* **2007**, *111*, 9595–9602.
(48) Chang, Y. T.; Hsu, S. L.; Chen, G. Y.; Su, M. H.; Singh, T. A.; Diau, E. W. G.; Wei, K. H. *Adv. Funct. Mater.* **2008**, *18*, 2356–2365.
(49) He, C.; He, Q. G.; Yang, X. D.; Wu, G. L.; Yang, C. H.; Bai, F. L.; Shuai, Z. G.; Wang, L. X.; Li, Y. F. *J. Phys. Chem. C* **2007**, *111*, 8661–8666.
(50) Kim, Y.; Choulis, S. A.; Nelson, J.; Bradley, D. D. C.; Cook, S.; Durrant, J. R. *J. Mater. Sci.* **2004**, 1371–1376.
(51) Zhou, Z. Y.; Chen, X. W.; Holdcroft, S. *J. Am. Chem. Soc.* **2008**, *130*, 11711–11718.
(52) Shaheen, S. E.; Brabec, C. J.; Sariciftci, N. S.; Padinger, F.; Fromherz, T.; Hummelen, J. C. *Appl. Phys. Lett.* **2001**, *78*, 841–843.
(53) Roquet, S.; Cravino, A.; Leriche, P.; Aleveque, O.; Frere, P.; Roncali, J. *J. Am. Chem. Soc.* **2006**, *128*, 3459–3466.
(54) Cravino, A.; Leriche, P.; Aleveque, O.; Roquet, S.; Roncali, J. *Adv. Mater.* **2006**, *18*, 3033–3037.
(55) Xia, P. F.; Feng, X. J.; Lu, J.; Tsang, S.-W.; Movileanu, R.; Tao, Y.; Wong, M. S. *Adv. Mater.* **2008**, *20*, 4810–4815.


MA900236H